Provided for non-commercial research and education use.
Not for reproduction, distribution or commercial use.

This article appeared in a journal published by Elsevier. The attached copy is furnished to the author for internal non-commercial research and education use, including for instruction at the authors institution and sharing with colleagues.

Other uses, including reproduction and distribution, or selling or licensing copies, or posting to personal, institutional or third party websites are prohibited.

In most cases authors are permitted to post their version of the article (e.g. in Word or Tex form) to their personal website or institutional repository. Authors requiring further information regarding Elsevier's archiving and manuscript policies are encouraged to visit:

http://www.elsevier.com/copyright

Author's personal copy

ELSEVIER

Available online at www.sciencedirect.com
ScienceDirect

Scripta Materialia 63 (2010) 422–425

www.elsevier.com/locate/scriptamat

# Strength distribution of single-crystal silicon theta-like specimens

Michael S. Gaither, Frank W. DelRio,* Richard S. Gates, Edwin R. Fuller, Jr. and Robert F. Cook

*Ceramics Division, Materials Science and Engineering Laboratory, National Institute of Standards and Technology, Gaithersburg, MD 20899, USA*

Received 5 February 2010; revised 23 March 2010; accepted 29 April 2010
Available online 5 May 2010

A new test specimen was developed for micro-scale tensile strength measurements, allowing direct assessment of surface effects on strength. Specimens were formed by deep reactive ion etching, tested with instrumented indentation, and test results interpreted using finite element analyses. Fracture strengths as great as 3 GPa were observed, with fracture initiating at processing-induced flaws and propagating along {1 1 1} and {1 1 0} planes.
Published by Elsevier Ltd. on behalf of Acta Materialia Inc.

*Keywords:* Finite element methods; Fracture strength; Microelectromechanical systems; Single-crystal silicon

The great potential for microelectromechanical systems (MEMS) is in devices that can perform significant mechanical work. Such work can be performed by MEMS that incorporate large-load components, such as thermal and piezoelectric actuators [1], or that include contacting and moving components, such as electrical contacts in microswitches, hinges in microactuators, and gear teeth in micromotors [2]. However, a possible consequence of the large loads and the frictional effects during device operation is that stress is generated in a component that exceeds the component strength, leading to component failure and thus truncated lifetime and uncertain device reliability. Careful fabrication procedures can lead to increased component strength (*e.g.*, the strength of single-crystal silicon structures and devices has been shown to reach values as great as 18 GPa [3]), but the distribution of strength values over component sample populations is usually extremely broad [4], and the stress ranges experienced in MEMS devices in use are likely to vary greatly. Thus, MEMS device reliability is difficult to predict, and as a result, the number of MEMS devices that demonstrate significant mechanical work is still limited.

A strategy to assess, predict, and optimize MEMS device reliability is to have a form of "proof test" [5]. Test structures to measure the strength of MEMS materials and components that could be used in proof testing or to optimize fabrication processes include tensile bars [6–8], fixed–free beams [9], fixed–fixed beams [3], and biaxial flexure plates [10]. To avoid the gripping, mounting, and loading misalignments that result in significant experimental errors in these geometries, Quinn et al. developed a micromachined "theta-like" test specimen [11,12], originally invented by Durelli et al. as a macro-scale test method [13], to measure strengths at the micro-scale. These test specimens, named for their likeness to the Greek letter $\Theta$, demonstrated the viability of the theta specimen technique, but also revealed a number of problems: mounting the specimens for testing was difficult, non-ideal loading led to undesirable stress concentrations, and collecting the broken parts after testing for fractography was difficult. In this paper, we describe a new arch theta test specimen for micro-scale tensile strength measurements. The new specimen was designed with a "top hat", fabricated using silicon-on-insulator (SOI) wafers, and tested using a break-detection routine to mitigate a number of the aforementioned problems.

The engineering drawing for the arch theta test specimen is shown in Figure 1 (dimensions are given in micrometer). The new design consists of an outer ring (250 μm diameter) with a central bar, or "web region", of uniform cross section (8 μm wide, 115 μm long). As with previous designs [11–13], the outer ring is diametrally compressed, thereby generating a uniaxial tensile stress state in the web region. In the new design, however, the top hat (80 μm wide, 45 μm tall) was included to minimize loading misalignments and stress concentrations [14], which result in stress gradients *across* the web

* Corresponding author. Tel.: +1 301 975 8999; fax: +1 301 975 5334; e-mail: frank.delrio@nist.gov

1359-6462/$ - see front matter Published by Elsevier Ltd. on behalf of Acta Materialia Inc.
doi:10.1016/j.scriptamat.2010.04.047

Author's personal copy



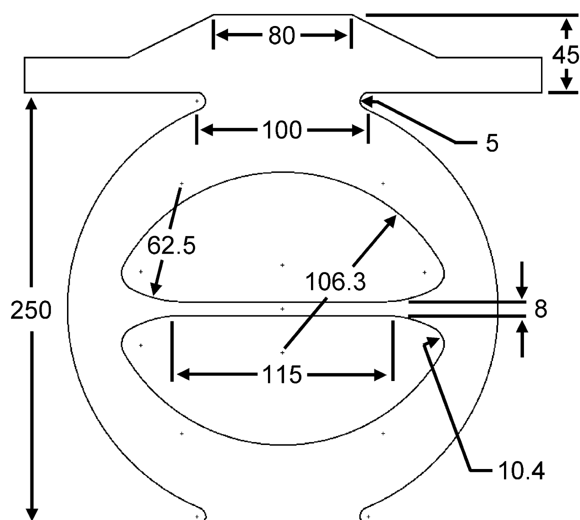


**Figure 1.** Engineering drawing of the arch theta test specimen (dimensions are given in micrometer).

region and primary fractures *outside* of the web region [11–13]. The complex inner geometry of the original Durelli theta design, which consisted of three straight sections linked by tangential radii, was also replaced with a simple arch (106.3 μm radius).

The fabrication sequence for the arch theta test specimen is shown in Figure 2. The process started with a (0 0 1) SOI wafer (100 mm diameter) consisting of a Si device layer (25.0 μm ± 0.5 μm thick), $SiO_2$ isolation layer (2.0 μm ± 0.1 μm thick), and a Si handle wafer (400 μm ± 10 μm thick). The SOI wafers allowed for

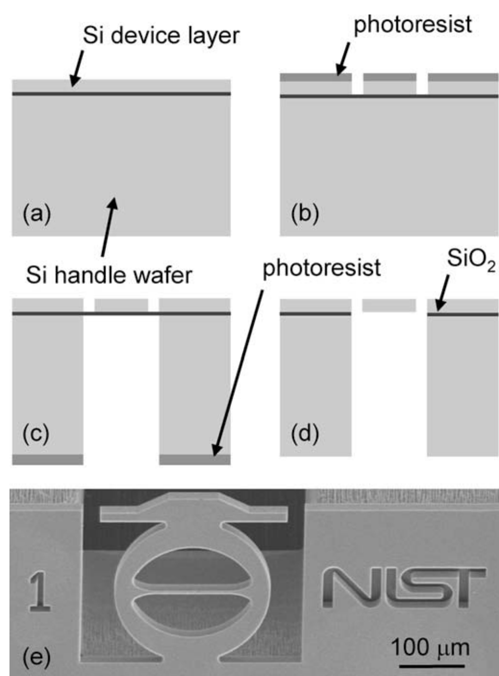


**Figure 2.** (a–d) Schematic diagrams of the fabrication sequence for the arch theta test specimen. (a) The process started with a SOI wafer. (b) The Si device layer and (c) Si handle wafer were patterned by a photolithographic mask and etched using DRIE to define the device features. (d) The $SiO_2$ layer was then removed locally with a buffered-oxide etching solution to create the freestanding structures. (e) Scanning electron micrograph of a completed device.

better control of device thickness and a more robust base for manipulation and mounting than in previous designs [11,12]. The Si device layer and Si handle wafer were patterned by photolithographic masks and etched using deep reactive ion etching (DRIE) to define the device features. The SOI wafer was positioned such that the web region of the test specimen was oriented along the <1 1 0> direction (the misalignment was found to be <0.5° by cleaving the SOI wafer and comparing the <1 1 0> cleavage line to the web regions of several arch theta test specimens). After Si etching, the $SiO_2$ layer was removed with a buffered-oxide etch to create the freestanding specimens. Finally, each specimen strip, which consisted of 10 test specimens, was removed from the wafer using a diamond scribe on notched regions at each end of the strip. The strips were mounted into a fixture using a clamping configuration that allowed the specimens to stand upright and remain isolated from the surrounding material. Each test specimen was then diametrally compressed via instrumented indentation using a spherical sapphire indenter tip (250 μm radius) and a break-detection routine that withdrew the indenter on detection of specimen failure to minimize subsequent damage. Fractography of the broken test specimens was conducted via field-emission scanning electron microscopy (FESEM) and the topography of the DRIE scallops was analyzed using atomic force microscopy (AFM).

Three-dimensional (3-D) finite element analysis (FEA) was used to convert the load $P$ and displacement $h$ at the indenter-to-sample interface to the stress σ and strain ε in the central web region. The 3-D FEA mesh consisted of ≈135,000 eight-node hexahedral elements. The average mesh size in the web region was about 2 μm; further refinements in the mesh were found to be unnecessary, as they did not improve the accuracy of the model. The elastic properties of silicon were modeled as cubic anisotropic with three independent second-order elastic coefficients $c_{11} = 165.8$ GPa, $c_{12} = 63.9$ GPa, and $c_{44} = 79.6$ GPa [15], and the sapphire indenter was modeled as an isotropic material with Young's modulus $E_{tip} = 400$ GPa and Poisson's ratio $\nu_{tip} = 0.24$ [16]. From the 3-D FEA, the largest maximum principal stress $\sigma_p$ occurred in the web region, and the largest secondary stress $\sigma_s$ was located at the top and bottom of the inner theta region. For the arch theta, the stress ratio of $\sigma_s/\sigma_p = 0.62$ confirmed that initial fracture should occur in the web region. σ (GPa) and ε were related to $P$ (mN) and $h$ (μm) by

$$\sigma = -14.38 \frac{P}{Dt}, \quad (1)$$

$$\varepsilon = -0.65 \frac{h}{D}, \quad (2)$$

where, $D$ is the arch theta diameter (μm) and $t$ is the device layer thickness (μm). Eqs. (1) and (2) are consistent with the idea that as the outer ring is diametrally compressed (negative $P$ and $h$), the central web region in placed in uniform tension (positive σ and ε). The equations are valid for the dimensions given in Figure 1 and the $P$ and $h$ ranges shown in Figure 3(a). The constants in each equation are different from those of the original Durelli theta test specimen [13] due to variations

Author's personal copy



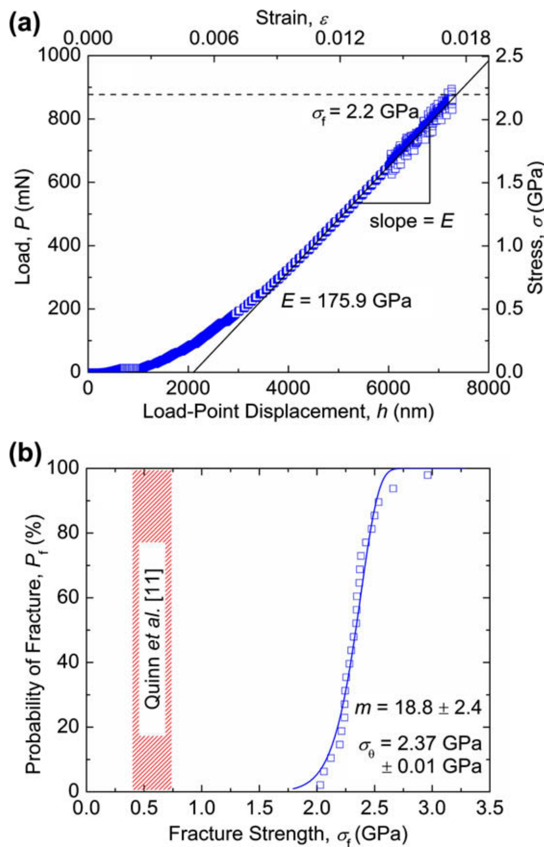


**Figure 3.** (a) Typical *P–h* data for an arch theta test specimen loaded to failure. $E$ and $\sigma_f$ for this specimen were 175.9 GPa and 2.2 GPa, respectively. (b) Weibull failure probability plot for the arch theta test specimen. The fracture strengths varied from 2.0 GPa to 3.0 GPa. $m$ and $\sigma_\theta$ were $18.8 \pm 2.4$ and 2.37 GPa $\pm$ 0.01 GPa, respectively, using a two-parameter Weibull distribution function (uncertainty values represent a 95% confidence level in the fit).

in the design (*e.g.*, arch shape for the top and bottom of the inner theta region, addition of the top hat).

Figure 3(a) illustrates a typical *P–h* curve for an arch theta test specimen loaded to failure. The initial non-linear region at small load was most likely due to the contacting and seating of the sapphire indenter sphere on the etched surface of the specimen. After the initial seating process, the *P–h* traces were linear with no discernable hysteresis during five unload–load cycles, which suggests the mounting and clamping configuration provides a secure and stable test platform. Young's modulus $E$ was determined from the slope of the linear portion of the σ–ε curve; for this particular specimen, $E = 175.9$ GPa, which is in good agreement with reported values for silicon in the <1 1 0> direction, $E = 168.9$ GPa [17]. The fracture strength, or the stress at which fracture occurred, was $\sigma_f = 2.2$ GPa. As fracture strength is limited by flaw size, a distribution of critical flaws from the fabrication sequence will result in a strength distribution. From Figure 3(b), the fracture strengths for 24 arch theta test specimens ranged from 2.0 GPa to 3.0 GPa. Such variability is often described by the two-parameter Weibull distribution function,

$$P_f = 1 - \exp\left(-\left(\frac{\sigma_f}{\sigma_\theta}\right)^m\right), \tag{3}$$

where, $P_f$ is the cumulative probability of failure, $\sigma_\theta$ is the characteristic strength, and $m$ is the Weibull modulus. To fit the data to Eq. (3), the strength values were ranked in ascending order from $i = 1$ to $N$, and a $P_f$ was assigned to each value according to $P_f = (i - 0.5)/N$, where $N = 24$ is the number of measurements. The Weibull parameters $m$ and $\sigma_\theta$ were then obtained via least squares fitting based on the Levenberg–Marquardt algorithm: $m$ and $\sigma_\theta$ were found to be $18.8 \pm 2.4$ and $2.37 \pm 0.01$ GPa, respectively (uncertainty values represent a 95% confidence level in the fit). These results are consistent with the ranges reported for micromachined single-crystal silicon: 0.5 GPa $< \sigma_f <$ 17.5 GPa, $2.7 < m < 62$, and 0.5 GPa $< \sigma_\theta <$ 17.6 GPa [4].

FESEM images of broken web regions revealed fractures originating on either {1 1 1} or {1 1 0} planes, which are the expected cleavage planes for single-crystal silicon [18]. In Figure 4(a), cleavage step hackle radiates from the fracture origin, which was chipped out during the fracture process. The critical flaw size $a_o$ can be estimated from

$$a_o = \left(\frac{K_{IC}}{Y\sigma_f}\right)^2, \tag{4}$$

where, $K_{IC}$ is the mode I fracture toughness and $Y$ is a shape factor. $K_{IC} = 0.71$ MPa m$^{1/2}$ for silicon on

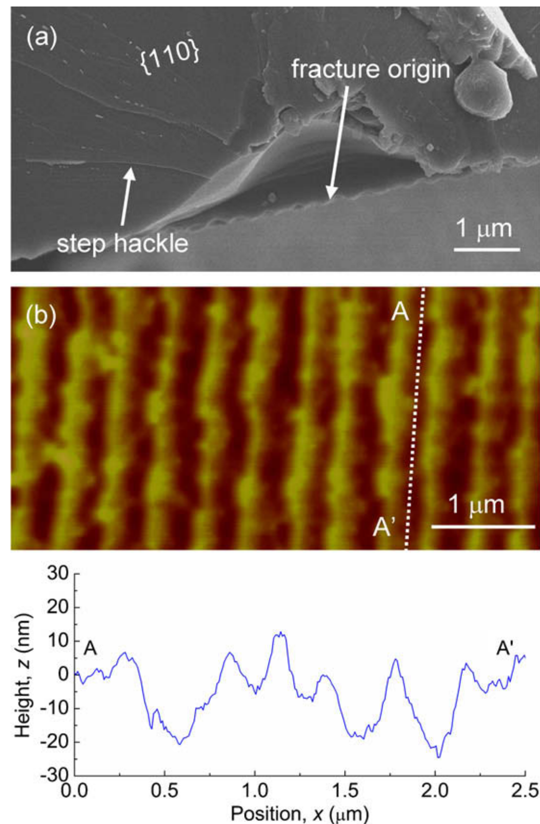


**Figure 4.** (a) FESEM image of the fracture surface for an arch theta test specimen. Fracture occurred on a {1 1 0} plane. The cleavage step hackle radiates from the fracture origin (arrow), which was chipped out during the fracture process. (b) AFM image of the DRIE scallops. The maximum perturbation along the length of the DRIE scallop (section AA′) is about 25 nm, which is similar to the calculated flaw sizes.

Author's personal copy



the {1 1 0} plane [18] and $Y \approx 1.12\pi^{1/2}$ for an edge crack in a semi-infinite solid [19]. From Figure 3(b), $\sigma_f$ varies from 2.0 GPa to 3.0 GPa, which results in $a_o$ values of about 30 nm to 10 nm, respectively. These calculated flaw sizes are comparable to the surface roughness along the length of the DRIE scallops (*i.e.*, the loading direction), as illustrated in Figure 4(b).

In summary, we reported on a new arch theta test specimen, which allowed for simple micro-scale strength testing, while removing the difficulties associated with gripping and loading specimens as well as minimizing potential misalignment effects. The fracture strengths for Si specimens ranged from 2.0 GPa to 3.0 GPa and the strength distribution was well-described by a two-parameter Weibull distribution function. The critical flaw sizes were calculated from the observed fracture strengths, and the resulting values suggested that processing-induced surface roughness acted as the strength-limiting flaws. Further studies are required to determine the relationship between calculated flaw sizes from strength measurements and surface roughness from the DRIE process.

The authors thank George D. Quinn of the National Institute of Standards and Technology for assistance and guidance with fractography.

[1] D.J. Bell, T.J. Lu, N.A. Fleck, S.M. Spearing, J. Micromech. Microeng. 15 (2005) S153.
[2] G.T.A. Kovacs, Micromachined Transducers Sourcebook, McGraw-Hill, New York, 1998.
[3] T. Namazu, Y. Isono, T. Tanaka, J. Microelectromech. Syst. 9 (2000) 450.
[4] O.M. Jadaan, N.N. Nemeth, J. Bagdahn, W.N. Sharpe Jr., J. Mater. Sci. 38 (2003) 4087.
[5] B.L. Boyce, R. Ballarini, I. Chasiotis, J. Micromech. Microeng. 18 (2008) 1.
[6] W.N. Sharpe, B. Yuan, R.L. Edwards, J. Microelectromech. Syst. 6 (1997) 193.
[7] W. Suwito, M.L. Dunn, S.J. Cunningham, D.T. Read, J. Appl. Phys. 85 (1999) 3519.
[8] B.L. Boyce, J.M. Grazier, T.E. Buchheit, M.J. Shaw, J. Microelectromech. Syst. 16 (2007) 179.
[9] F. Ericson, J.-A. Schweitz, J. Appl. Phys. 68 (1990) 5840.
[10] K.-S. Chen, A. Ayon, S.M. Spearing, J. Am. Ceram. Soc. 83 (2000) 1476.
[11] G.D. Quinn, E. Fuller, D. Xiang, A. Jillavenkatesa, L. Ma, D. Smith, J. Beall, Ceram. Eng. Sci. Proc. 26 (2005) 117.
[12] G.D. Quinn, Ceram. Eng. Sci. Proc. 29 (2008) 189.
[13] A.J. Durelli, S. Morse, V. Parks, Mater. Res. Stand. 2 (1962) 114.
[14] E.R. Fuller, D.L. Henann, L. Ma, Int. J. Mater. Res. 98 (2007) 729.
[15] H.J. McSkimin, P. Andreatch Jr., J. Appl. Phys. 35 (1964) 3312.
[16] B. Holm, R. Ahuja, Y. Yourdshahyan, B. Johansson, B.I. Lundqvist, Phys. Rev. B 59 (1999) 12777.
[17] W.A. Brantley, J. Appl. Phys. 44 (1973) 534.
[18] R.F. Cook, J. Mater. Sci. 41 (2006) 841.
[19] B. Lawn, Fracture of Brittle Solids, Cambridge University Press, Cambridge, 1993.